

## Spin Transition Evidenced by Soft X-ray Absorption Spectroscopy

Christophe Cartier dit Moulin,<sup>\*,†</sup> Petra Rudolf,<sup>‡,§</sup> Anne-Marie Flank,<sup>†</sup> and Chien-Te Chen<sup>†</sup>

LURE, Bâtiment 209d, F-91405 Orsay, France, and AT&amp;T Bell Laboratories, Murray Hill, New Jersey 079074 (Received: January 14, 1992; In Final Form: March 31, 1992)

Iron  $L_{2,3}$  X-ray absorption spectra have been recorded in order to follow the thermal reversible spin interconversion of the  $\text{Fe}^{\text{II}}(\text{phen})_2(\text{NCS})_2$  (phen = *o*-phenanthroline). Important differences are observed which show that this spectroscopy is a fingerprint of the spin state. The evolution of the branching ratio is discussed and found to be consistent with the expected value obtained by multiplet calculations.

## Introduction

In a number of transition-metal molecular compounds, the ligand field strength is of the same order of magnitude as the average electron pairing energy. The metal ion is then capable of undergoing a spin-state interconversion under the effect of an external perturbation such as a temperature change. Compounds that present this kind of reversible spin transition could be useful for electronic devices (switching, signal processing, data storage). The understanding of the transition mechanism is essential for the design of new compounds in the molecular electronic field.

It has been shown previously that, in the case of  $\text{Ni}^{2+}$  compounds, metal  $L_{2,3}$  X-ray absorption (XAS) spectra can be used as a fingerprint for the spin state.<sup>1</sup> For other 3d transition metals the situation is more complicated, but the XAS spectra nevertheless provide an unambiguous determination of the spin state<sup>2-4</sup> and allow also a precise measurement of the  $10Dq$  parameter in the compounds. In the case of spin-transition compounds, the knowledge of this parameter and of its variation during the transition is extremely important for the understanding of the phenomenon and for the design of new compounds.

The electronic structure of the 3d transition metals is strongly determined by the filling of the 3d states.  $L_{2,3}$  absorption spectroscopy is a fundamental probe of the empty 3d states because of the very restrictive electric dipole selection rules: the main dipole-allowed transition is  $2p \rightarrow nd$  mixed with a small amount of  $2p \rightarrow ns$ . The configuration of the 3d valence states in iron compounds is influenced by the oxidation state as well as by the local environment (symmetry, nature of the ligand, and metal-ligand distances). Another important parameter is the spin state which depends mainly on the chemical environment and which involves directly the d levels.<sup>1</sup> Preliminary experiments performed on a two-crystal monochromator equipped with a W/C multilayer/KAP combination already revealed the sensitivity of the iron  $L_3$  and still more of the  $L_2$  edge to the spin state.<sup>5</sup> The disadvantages of working with such an experimental setup are the weak performance of the radiation-damaged KAP crystals and the poor resolution of the system limited by the use of a KAP as the second crystal. The new generation of soft X-ray synchrotron radiation monochromators like the AT&T Bell Laboratories' Dragon<sup>6-8</sup> at the National Synchrotron Light Source (NSLS) with its high-energy resolution gives access to spectra measured with great accuracy. They appear very powerful for those cases where the absorption spectra exhibit a lot of fine structure due to atomic multiplet and crystal-field effects.

In this paper, we report on a reversible spin transition, studied and thermocontrolled "in situ" of  $\text{Fe}^{\text{II}}(\text{phen})_2(\text{NCS})_2$  (phen = *o*-phenanthroline). This compound crystallizes in an  $O_h$  symmetry. In such an octahedral environment, the 5-fold degenerated 3d orbitals are divided into two distinct representations of  $T_{2g}$  and  $E_g$  symmetry with 3- and 2-fold degeneracy, respectively. The

$\text{Fe}^{\text{II}}(\text{phen})_2(\text{NCS})_2$  presents an abrupt spin transition  $t_{2g}^4 e_g^2 [S=2] \rightarrow t_{2g}^6 e_g^0 [S=0]$  which is complete at  $T = 170$  K. In the high-spin ground state—and for an octahedral environment—the higher lying orbitals are occupied with the spins oriented in the same direction ( $(t_{2g})^4 (e_g)^2$  configuration), while in the low-spin ground state the electrons pair up in the orbitals with the lowest energy ( $(t_{2g})^6 (e_g)^0$  configuration). An EXAFS analysis of the iron K edge<sup>9</sup> revealed a contraction of the first coordination shell of  $\Delta R = 0.24$  Å when the metallic ion transits from the high-spin to the low-spin state. An increase of the Debye-Waller factor has also been observed in the low-spin (low-temperature) configuration. This structural change characterized by EXAFS has been recently confirmed by a single-crystal X-ray investigation.<sup>10</sup> The decrease of the volume of the coordination sphere corresponds to an increase in the ligand field parameter ( $10Dq$ ) which is an important parameter in the theory describing the transitions  $2p^6 3d^n \rightarrow 2p^5 3d^{n+1}$ . If this increase in crystal-field strength is large enough, the further decrease in the energy level of the  $t_{2g}$  symmetry could overcome the energy increase due to spin-spin interaction going from  $S = 2$  to  $S = 0$  and thus favor the low-spin ( $t_{2g})^6 (e_g)^0$  configuration.

## Experimental Section

**Compound Preparation.** The different methods for the spin-transition complex  $\text{Fe}^{\text{II}}(\text{phen})_2(\text{NCS})_2$ <sup>11,12</sup> produce samples which yield identical powder diffraction as well as infrared (IR) spectra but differ in the size of the single crystals. In order to get a sharp transition, we chose the preparation method leading to the largest well-developed single crystals.<sup>12</sup> The compound is obtained by extracting a phenanthroline ligand from  $\text{Fe}(\text{phen})_3(\text{NCS})_2$  in a liquid extractor Soxhlet, by using acetone. The synthesis lasts over 3 weeks, under controlled argon atmosphere. Successively the purple crystals are dried under vacuum over  $\text{P}_2\text{O}_5$ . Once prepared, the complex is stable at room temperature. The quality of the products was controlled by IR spectroscopy and microanalysis. Furthermore, the variation of the magnetic susceptibility was measured as a function of the temperature. The result is shown in Figure 1 and gives a good indication for a complete high/low-spin interconversion  $S = 2 \leftrightarrow S = 0$  at  $T = 176$  K.

During the bake-out of the experimental chamber for the XAS measurements, the sample was water cooled to prevent an alteration of the compound. For the measurements at 77 K, the sample temperature was lowered at a rate of 2 K/min to avoid a quenching of the spin state.

**Experimental Setup for XAS Measurements.** The design and the performance of the Dragon beam line have been discussed previously.<sup>6-8</sup> The spectra were measured by total electron yield detection. The absolute photon energy scale was calibrated using the value of 708.5 eV for the maximum of the  $L_3$  line in  $\text{Fe}_2\text{O}_3$  and checked before and after each measurement of the sample. For the energy range of the Fe  $L_{2,3}$  edges (700–730 eV), photon energy resolution was set at an expected value of 0.24 eV full width at half-maximum (fwhm) using 0.25- $\mu\text{m}$  entrance and exit slits. This value is calculated taking into account the effect of finite slit opening, optical aberration, and grating figure errors, the latter being the dominant factor limiting the resolution.<sup>13</sup> The shape

<sup>\*</sup> LURE.<sup>†</sup> AT&T Bell Laboratories.<sup>‡</sup> Permanent address: Laboratorio T.A.S.C.-I.N.F.M., Padriciano 99, I-34012 Trieste, Italy.

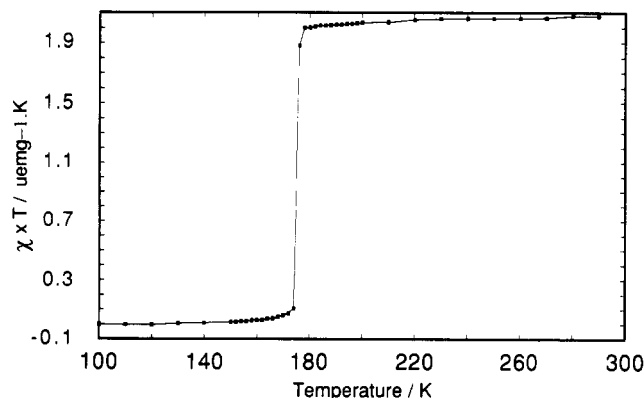


**Figure 1.** Temperature dependence of the  $\chi_m T$  for the  $\text{Fe}(\text{phen})_2(\text{NCS})_2$  sample. (The magnetic susceptibility measurements were performed over the temperature range 295–77 K, by using a Faraday type magnetometer equipped with a continuous-flow cryostat.)

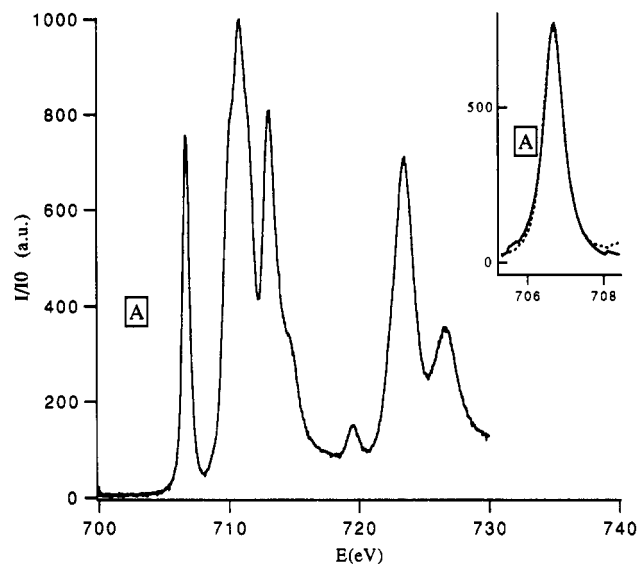


**Figure 2.**  $\text{Fe } L_{2,3}$  edges in  $\text{K}_3\text{Fe}^{\text{III}}(\text{CN})_6$ . The peak labeled "A" can be considered as corresponding to a singlet excitation ( $2p_{3/2}t_{2g}^5 \rightarrow 2p_{3/2}t_{2g}^6$  transition). Insert is a comparison between peak A (---) and a fit by a Lorentzian line shape (—).

of the instrumental broadening has been discussed previously,<sup>14</sup> without reaching any definite conclusion on whether pure Gaussian or pure Lorentzian forms should be assumed. The other major factor limiting the amount of information which can be extracted from the absorption spectra is the Lorentzian broadening due to the core-hole lifetime. A semiempirical evaluation<sup>15</sup> for the natural widths of atomic Fe  $L_3$  edge gives 0.36 eV with an uncertainty of about 20% since many-body effects are not considered. The total expected broadening results therefore from a convolution of a Gaussian (experimental) and a Lorentzian (core hole lifetime) profile, with respective widths  $\sigma_G$  and  $\sigma_L$ , and has a "Voigt" profile with a fwhm given by  $\sigma_V^2 = (\sigma_L^2 + \sigma_G^2/\ln 2)$ .

To get an idea of the total experimental broadening, we measured Fe  $L_{2,3}$  edges in  $\text{K}_3\text{Fe}^{\text{III}}(\text{CN})_6$  in octahedral symmetry which has the low-spin  $t_{2g}^5 e_g^0$  configuration in the ground state. The spectrum is plotted in Figure 2 and shows two peaks at the  $L_3$  edge: the first feature labeled "A" corresponds to the singlet excitation  $2p_{3/2}t_{2g}^5 \rightarrow 2p_{3/2}t_{2g}^6$ . This sharp peak can be well fitted with both a Lorentzian and a Gaussian line shape and has a line width of 0.63 eV. Comparing this value to the expected width  $\Delta E = ((0.24)^2/\ln 2 + (0.36)^2)^{1/2} = 0.46$  eV (or  $\Delta E = 0.24 + 0.36 = 0.6$  eV by assuming a Lorentzian instrumental broadening), one notes an extra broadening of vibrational or thermal origin (solid-state effect).<sup>16</sup> The second peak which corresponds to the transition from  $2p_{3/2}$  to empty  $e_g$  orbitals exhibits at least five structures, which have to be analyzed with a multiplet model taking into account the exchange interaction between the 2p hole

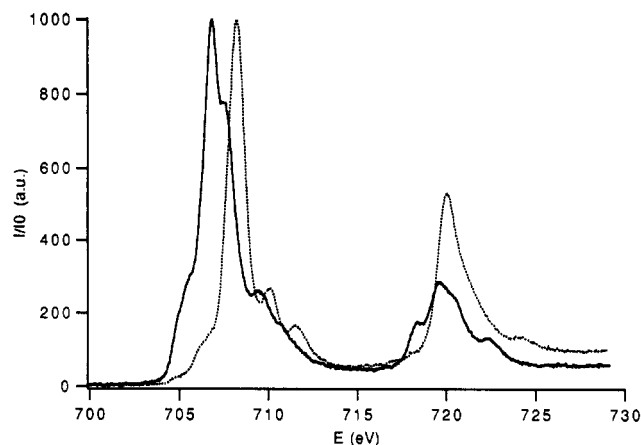


**Figure 3.** Experimental  $L_{2,3}$  absorption spectra of  $\text{Fe}(\text{phen})_2(\text{NCS})_2$  at 300 K (—) (high-spin configuration  $S = 2$ ) and 77 K (---) (low-spin configuration  $S = 0$ ).

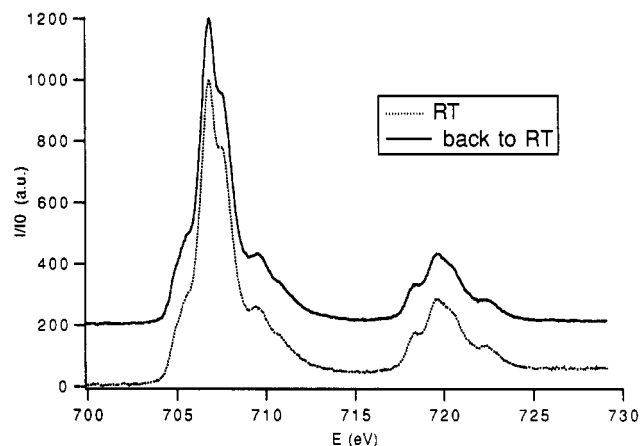


**Figure 4.** Comparison of the  $L_{2,3}$  absorption spectra of  $\text{Fe}(\text{phen})_2(\text{NCS})_2$  at 300 K (---) before and (—) after the spin transition.

and 3d electrons.<sup>17</sup> Note that the splitting of the  $L_3$  line is related, but not directly scaled, to the  $10Dq$  crystal field strength parameter (energy separation between the levels  $t_{2g}$  and the center of mass of the  $e_g$  levels).

## Results and Discussion

Figure 3 shows the Fe  $L_{2,3}$  edges of the spin-transition complex  $\text{Fe}^{\text{II}}(\text{phen})_2(\text{NCS})_2$  recorded at 300 and 77 K. There are very marked differences between the two spectra: at 77 K the whole spectrum is shifted to higher energies (1.44 eV for the  $L_3$  maximum and 0.5 eV for the  $L_2$ ), and the  $L_3$  peak presents better resolved structures. The  $L_2$  white line which presents three well-resolved features at 300 K becomes simplified at low temperatures and increases strongly in intensity. We have observed in other iron compounds<sup>18</sup> that such a shape for the  $L_2$  peak is the signature of a low-spin configuration.

Figure 4 compares the initial Fe  $L_{2,3}$  spectrum to the one obtained after the full cycle, i.e., after cooling from 300 K and heating again to room temperature, and evidences the complete reversibility of the spin transition.

The important differences in the spectra corresponding to the two spin states reflect not only the modifications of the ground-state configuration but also that of the final state. A complete interpretation of both spectra would require complete multiplet calculations which in the case of  $\text{Fe}^{2+}$  ions where six electrons have to be accommodated in five 3d orbitals in an octahedral surrounding are complicated. The crystal-field multiplet program (developed by B. T. Thole) takes all interactions within the  $2p^5 3d^{n+1}$  final states into account simultaneously.

Let us now turn our attention to the variation in relative intensity of the two L edges with the spin transition. Atomic calculations have shown that the branching ratio, defined as the fraction of the total line strength going into a given  $j$  manifold,

is not equal to the statistical value, which is the total fraction of final states in that manifold, but depends linearly on both the valence band spin-orbit coupling and the interactions in the final state.<sup>19</sup> Therefore, it probes directly the character of the ground-state valence-band spin-orbit splitting in transition-metal compounds.

For dipole transitions  $2pd^n \rightarrow 2pd^{n+1}$ , if the local angular momentum  $j$  of the core hole is an exact quantum number in the final state  $\Psi$ , the total multiplet contribution to the  $L_3$  or  $L_2$  peak can be written as<sup>19</sup>

$$B_j(\Psi) = B^0 \pm A \langle \Psi | Z | \Psi \rangle \quad (1)$$

where the  $\pm$  sign is for  $j = l \pm 1/2$ . The first term  $B^0$  gives the statistical value. The proportionality constant  $A$  depends only on the specific transition and on the number of electrons  $n$  ( $A = -1/12$  in our case).  $Z = \sum_i \vec{l}_i \cdot \vec{s}_i$  is the spin-orbit operator.

At low temperature, where the spin state of the iron compound considered is  $S = 0$ , the spin-orbit operator is equal to 0. Therefore, the branching ratio amounts to the statistical value which is equal to 0.66. Calculating the respective areas of the  $L_2$  and the  $L_3$  peak in the 77 K spectrum of  $\text{Fe}^{\text{II}}(\text{phen})_2(\text{NCS})_2$ , we obtain an experimental value for the branching ratio equal to 0.67, in very good agreement with the theory.

We can now predict the evolution of the branching ratio with the  $S = 0 \rightarrow S = 2$  transition. At room temperature, for  $S = 2$ , the spin-orbit operator contribution to the branching ratio is different from zero. The exact calculation of the matrix element  $\langle \Psi | Z | \Psi \rangle$  is difficult and lies beyond the aims of this work. However, within the free atom approximation, we can predict the sign of the second term in eq 1: the proportionality constant  $A$  is always negative, and  $\langle \Psi | Z | \Psi \rangle$  has the sign of the effective spin-orbit factor/spin-orbit parameter ratio (relation given in ref 19), which for a  $d^6$  high-spin configuration is always negative. We therefore expect an increase in the branching ratio on going from the low-spin to the high-spin configuration.

Experimentally, we computed from peak areas in the 300 K spectrum a branching ratio of 0.79 for the  $S = 2$  spin state, in agreement with the predicted evolution. The branching ratio for 3d metals has been calculated<sup>20,21</sup> for all configurations and all the  $J$  levels of the Hund's rule ground-state LS terms within the free atom approximation, yielding a value of 0.78 for a  $d^6$  ( $S = 2$ ,  $J = 4$ ) configuration. The spin-orbit expectation value, computed from crystal-field theory, increases the branching ratio by 0.044. Hence, the experimental value falls between the two theoretical ones (with and without the crystal-field effect). This agreement appears fairly good, taking into account the uncertainty in the experimental determination of the branching ratio.

## Conclusion

We have demonstrated that the  $L_{2,3}$  transition-metal edges are a good fingerprint of the spin state and can be used to evidence an interconversion between two different spin states.

The crystal-field multiplet calculations developed by Thole need further theoretical developments to be applied to covalent systems such as the cyanide complexes and to extract the crystal-field parameters from XAS spectra.

**Acknowledgment.** We give special thanks to Ch. Brouder for fruitful discussions and to F. Sette for his interest and continuous support. We also thank E. Prouzet from the Institut des Matériaux de Nantes for the magnetic susceptibility measurements. P.R. acknowledges the financial support by the C.N.R., Rome, Italy. Work done at the National Synchrotron Light Source was supported by the U.S. DOE under Contract DA-ACO2-76CH00016.

## References and Notes

- (1) Van der Laan, G.; Thole, B. T.; Sawatzky, G. A.; Verdaguer, M. *Phys. Rev. B* **1988**, *37*, 6587.
- (2) Van der Laan, G.; Bruijn, M. P.; Goedkoop, J. B.; Mac-Dowel, A. A. *Proc. Photo-Opt. Instrum. Eng.* **1987**, *733*, 354.
- (3) Van der Laan, G.; Goedkoop, J. B.; Mac-Dowel, A. A. *J. Phys. E* **1987**, *20*, 1496.
- (4) Cramer, S. P.; De Groot, F. M. F.; Ma, Y.; Chen, C. T.; Sette, F.; Kipke, C. A.; Eichhorn, D. M.; Chan, M. K.; Armstrong, W. H.; Libby, E.; Christou, G.; Brooker, S.; McKee, V.; Mullins, O. C.; Fuggle, J. C. *J. Am. Chem. Soc.* **1991**, *113*, 7937.
- (5) Cartier, C.; Flank, A. M. *X-ray Absorption Fine Structure*; Hasnain, S., Ed.; Ellis Horwood: London, 1991; p 659.
- (6) Chen, C. T.; Sette, F. *Rev. Sci. Instrum.* **1989**, *60*, 1616.
- (7) Chen, C. T.; Sette, F. *Phys. Scr.* **1990**, *T31*, 119.
- (8) Sette, F.; Sinkovic, B.; Ma, Y. J.; Chen, C. T. *Phys. Rev. B* **1989**, *39*, 11125.
- (9) Cartier, C.; Thuery, P.; Verdaguer, M.; Zarembowitch, J.; Michalowicz, A. *J. Phys. (Paris)* **1986**, *47*, C8-563.
- (10) Gallois, B.; Real, J. A.; Hauw, C.; Zarembowitch, J. *Inorg. Chem.* **1990**, *29*, 1152.
- (11) Ganguli, P.; Gütlich, P.; Müller, E. W.; Irlner, W. *J. Chem. Soc., Dalton Trans.* **1981**, 441.
- (12) Madeja, K.; Wilke, W.; Schmidt, S. Z. *Anorg. Allg. Chem.* **1966**, *346*, 306.
- (13) Chen, C. T. *Nucl. Instrum. Methods A* **1987**, *256*, 595.
- (14) Kortboyer, S. W.; Goedkoop, J. B.; De Groot, F. M. F.; Grioni, M.; Fuggle, J. C.; Petersen, H. *Nucl. Instrum. Methods A* **1989**, *275*, 435.
- (15) Krause, M. O.; Oliver, J. H. *J. Chem. Phys. Ref. Data* **1979**, *8*(2).
- (16) De Groot, F. M. F.; Fuggle, J. C.; Thole, B. T.; Sawatzky, G. A. *Phys. Rev. B* **1990**, *41*, 928.
- (17) De Groot, F. M. F.; Fuggle, J. C.; Thole, B. T.; Sawatzky, G. A. *Phys. Rev. B* **1990**, *42*, 5459.
- (18) Cartier, C.; et al. To be published.
- (19) Thole, B. T.; Van der Laan, G. *Phys. Rev. A* **1988**, *38*, 1943.
- (20) Van der Laan, G. *Physica B* **1989**, *158*, 395.
- (21) Van der Laan, G.; Thole, B. T. *Phys. Rev. Lett.* **1988**, *60*, 1977.